Current Biology, Vol. 15, 955–962, May 24, 2005, ©2005 Elsevier Ltd All rights reserved. DOI 10.1016/j.cub.2005.04.054

Lethal Giant Larvae Controls the Localization of Notch-Signaling Regulators Numb, Neuralized, and Sanpodo in *Drosophila* Sensory-Organ Precursor Cells

Johanna Langevin,[1,4] Roland Le Borgne,[2,4] François Rosenfeld,[1] Michel Gho,[3] François Schweisguth,[2,*] and Yohanns Bellaïche[1,*]
[1]Institut Curie
Unité mixte de recherche 144
26 rue d'Ulm
75248 Paris cedex 05
France
[2]Ecole Normale Supérieure
Unité mixte de recherche 8542
46 rue d'Ulm
75005 Paris
France
[3]Université Paris VI
Centre National de la Recherche Scientifique
Unité mixte de recherche 7622
9 Quai St. Bernard
75005 Paris
France

Summary

Asymmetric distribution of fate determinants is a fundamental mechanism underlying the acquisition of distinct cell fates during asymmetric division. In *Drosophila* neuroblasts, the apical DmPar6/DaPKC complex inhibits Lethal giant larvae (Lgl) to promote the basal localization of fate determinants [1–3]. In contrast, in the sensory precursor (pI) cells that divide asymmetrically with a planar polarity, Lgl inhibits Notch signaling in the anterior pI daughter cell, pIIb, by a yet-unknown mechanism [4]. We show here that Lgl promotes the cortical recruitment of Partner of Numb (Pon) and regulates the asymmetric distribution of the fate determinants Numb and Neuralized during the pI cell division. Analysis of Pon-GFP and Histone2B-mRFP distribution in two-color movies confirmed that Lgl regulates Pon localization. Moreover, posterior DaPKC restricts Lgl function to the anterior cortex at mitosis. Thus, Lgl functions similarly in neuroblasts and in pI cells. We also show that Lgl promotes the acquisition of the pIIb cell fate by inhibiting the plasma membrane localization of Sanpodo and thereby preventing the activation of Notch signaling in the anterior pI daughter cell. Thus, Lgl regulates cell fate by controlling Pon cortical localization, asymmetric localization of Numb and Neuralized, and plasma-membrane localization of Sandopo.

Results and Discussion

The pI cell divides asymmetrically within the plane of the dorsal thorax (notum) epithelium to produce the posterior pIIa cell and the anterior pIIb cell, which go on to generate the external and internal cells of the adult mechanosensory organs, respectively (Figures 1A and 1B) [5–7]. The planar polarity of the pI cell division is marked by the anterior asymmetric localization of the cell-fate determinants Neuralized (Neur), Numb, and Numb's adaptor, Pon, which then segregate into the anterior pI daughter cell [5, 8–10]. Numb inhibits Notch (N) signaling in the anterior cell that therefore adopts the pIIb fate [11, 12]. Neur promotes Delta (Dl) endocytosis and activity in the anterior cell and thereby promotes N activation in the posterior cell, which therefore becomes pIIa [10].

The anterior asymmetric localizations of Neur, Numb and Pon are dependent upon the protein Pins [10, 13, 14]. Pins localizes at the anterior pI cortex, opposite to the *Drosophila* components of the Par complex, Bazooka (Baz, also known as D-Par3), DaPKC, and DmPar6 ([13, 15]; Figure 1B; and data not shown). Pins restricts the localization of Baz to the posterior cortex of the dividing pI cell [13]. In turn, Baz promotes the asymmetric localization of Numb, Pon, and probably Neur at the anterior pI cortex [13, 15]. The mechanisms by which Baz regulates the localization of both Numb and Pon are currently unknown.

The product of the tumor-suppressor gene *lgl* plays a key function in the binary pIIa/pIIb cell-fate decision in the pI lineage [3, 4]. Lgl is also required for the unequal segregation of fate determinants in dividing *Drosophila* neuroblasts [1–3]. However, Lgl has recently been reported to be dispensable for the asymmetric localization of Numb and Pon-GFP in dividing pI cells [4]. We therefore speculated that Lgl may act to regulate the asymmetric distribution of Neur in dividing pI cells. Accordingly, Lgl would act to prevent the posterior cell from inheriting Neur and, therefore, from activating Dl in this cell and N receptor signaling in the anterior one. To test this hypothesis, we compared the localizations of Neur, Numb, and Pon in dividing wild-type pI cells and dividing pI cells mutant for the lgl^4 null allele. Neur formed a crescent at the anterior cortex of wild-type pI cells in prometaphase or metaphase (n = 10, Figure 1C). Strikingly, Neur failed to form a crescent at the anterior cortex in 57% of the *lgl* mutant pI cells in prometaphase or metaphase (n = 7) and within 64% of the *lgl* mutant pI cell in telophase (n = 15, Figure 1D and not shown). Immunolocalization of Numb and Pon revealed that both Numb and Pon formed a crescent at the anterior cell cortex of wild-type pI cells in prometaphase (Figures 1E and 1F, n = 28 for Numb and n = 42 for Pon). However, Numb, like Neur, either failed to localize asymmetrically or formed a very faint crescent at the anterior cortex in 69% of the *lgl* mutant pI cells in prometaphase or metapahase (n = 23, Figure 1E) and in 66% of the *lgl* pI cells in telophase (n = 18, not shown). Similarly, Pon asymmetric localization was disrupted in 73% of the *lgl* mutant pI cells in prometaphase or metaphase (n = 37) and in 44% of *lgl* mutant pI cell in anaphase or telophase (n = 9, not shown). Importantly, Pon was detected in the cytoplasm of the dividing *lgl* mutant pI cells (Figure 1G), indicating that Lgl is needed

*Correspondence: yohanns.bellaiche@curie.fr (Y.B.); schweisg@wotan.ens.fr (F.S.)
[4]These authors contributed equally to this work.

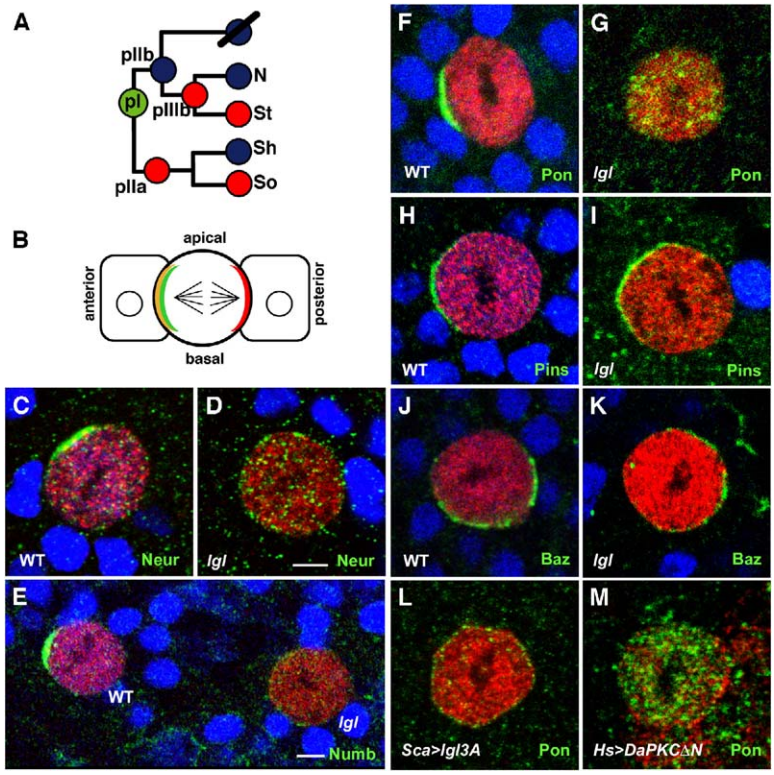

Figure 1. Lgl Regulates Asymmetric Localization of Neur, Numb, and Pon

(A) Wild-type sensory-organ cell lineage [6, 7]. N signaling is activated in the cell depicted in red. A stereotyped series of four asymmetric divisions generates a presumptive glial cell that undergoes apoptosis [6], the internal sensory cells, the neuron (Ne), and the sheath cell (St), as well as the external sensory cells, the shaft cell (Sh), and the socket cell (So).

(B) Diagram showing the polar distribution of the Baz-DmPar6-DaPKC complex (red), of the Pins-Gαi complex (orange), and of the cell-fate determinants Neur, Numb, and its adaptor Pon (green) in a dividing pI cell [13–15]. The pI cell divides within the plane of the epithelium and along the anterior-posterior axis [5].

(C–K) Localization of Neur (green in [C] and [D]), Numb (green in [E]), Pon (green in [F] and [G]), Pins (green in [H] and [I]), and Baz (green in [J] and [K]) at prometaphase in wild-type ([C], left cell in [E]; [F], [H], [J]) and *lgl*^{4} mutant ([D], right cell in [E]; [G], [I], [K]) pI cells. pI cells were identified by Senseless (Sens) staining (red). The *lgl* mutant pI cells were identified by the loss of nls-GFP staining (blue). The cell cycle was determined by DAPI counterstaining (not shown).

(L) Localization of Pon (green) in a dividing pI cell was identified by Sens staining (red) in the notum of pupae expressing *lgl3A* under the control of *scabrous*^{cPGAL4}.

(M) Localization of Pon (green) in a dividing pI cells overexpressing *DaPKCΔN* under the control of the *hs-GAL4* driver was identified by Sens staining (not shown) and DaPKC staining (red). Four hours prior to dissection, pupae were heat shocked for 45 min at 37°C. Wild-type pupae and pupae expressing wild-type *DaPKC* under the control of the hs-GAL4 driver were heat shocked in parallel and used as controls. Note that the accumulation of *DaPKCΔN* is not uniform. Anterior is on the left. The scale bar represents 5 μm.

for Pon cortical localization in dividing pI cells. In contrast, the localization of both Baz at the posterior cortex and Pins at the anterior cortex of the dividing *lgl* mutant pI cells was indistinguishable from that observed in adjacent dividing wild-type pI cells (n = 10 for Pins, Figures 1H and 1I and n = 8 for Baz, Figures 1J and 1K). These results indicate that Lgl acts downstream of or parallel to Baz and Pins to regulate the asymmetric localization of Numb and Neur and the cortical localization of Pon during the pI cell division.

In the dividing neuroblasts of the *Drosophila* embryo, Lgl is uniformly cortical, and the apical DaPKC kinase restricts the Lgl activity to the basal neuroblast cortex by phosphorylation on three conserved serines [1–3]. In support of this model, the overexpression of *lgl3A* (a nonphosphorylable mutant form of *lgl)* was found to promote uniform cortical recruitment of Numb, Prospero, Pon, and Miranda in the dividing neuroblasts [1]. Additionally, the overexpression of *DaPKCΔN*, a constitutively active form of *DaPKC*, leads to a phenotype similar to the one observed in the *lgl* mutant neuroblasts, i.e., a delocalization of Miranda from the basal cortex to the cytoplasm [1]. In dividing pI cells, DaPKC and DmPar6 are localized with Baz at the posterior cortex, and Lgl is uniformly cortical ([4, 13, 15] and data not shown). In order to test whether the phosphorylation of Lgl by DaPKC restricts the activity of Lgl to the anterior pI cell cortex, we overexpressed the *lgl3A* mutant form by using the Gal4/UAS system [16]. In dividing pI cells, the overexpression of wild-type *lgl* did not affect the localization of Numb (n = 22) or Pon (n = 16; not shown). In contrast, the overexpression of the *lgl3A* mutant form affected the localization of Pon in 70% of the dividing pI cells (n = 18, Figure 1L). Pon uniformly localized to the cortex in 36% of the cells or localized to the cortex with a weak anterior accumulation in 34% of the dividing pI cells overexpressing the *lgl3A* form. Similarly, a loss of asymmetric Numb and Neur localization was observed upon overexpression of *lgl3A* (Numb: n = 22, 18% uniformly cortical and 36% cortical with a weak anterior accumulation. Neur: n = 26, 63% uniformly cortical and 36% cortical with a weak anterior accumulation). The overexpression of the constitutively active form *DaPKCΔN* resulted in the cytoplasmic localization of Pon in 80% of the dividing pI cells where DaPKCΔN was detectable (n = 12, Figure 1M). This phenotype is similar to the one observed in the dividing *lgl* mutant pI cells, indicating that the activity of Lgl is inhibited by DaPKC. We propose that the Par complex blocks the activity of Lgl at the posterior cortex of the pI cell and thereby promotes the localization of Pon, Numb, and Neur at the opposite anterior cortex.

The dynamics of Pon-GFP localization were also analyzed in living pupae. At interphase, Pon-GFP accumulated at the cortex and in the nucleus of wild-type pI cells (Figures 2A and 2C). In contrast, in *lgl* mutant pI cells in interphase (n > 30), Pon-GFP accumulated to high levels within the nucleus and was almost absent

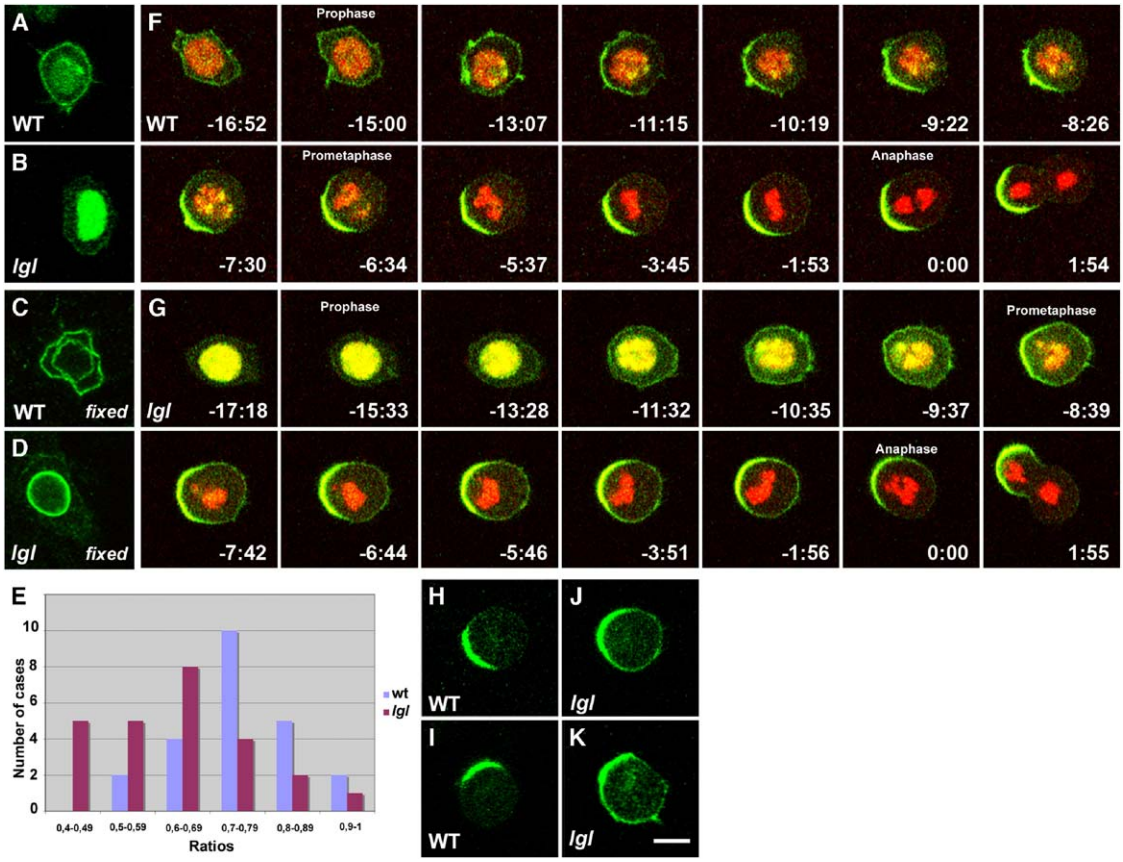

Figure 2. Asymmetric Localization of Pon-GFP Is Delayed in *lgl* Mutant pI Cells

(A and B) Interphasic localization of Pon-GFP expressed under the control of $neur^{PGAL4}$ in wild-type (A) and lgl^{4} mutant (B) pI cells in living pupae.

(C and D) Interphasic localization of Pon-GFP (green) in a wild-type (C) and a lgl^{4} mutant (D) fixed pI cell. Note that upon fixation the nuclear pool of Pon-GFP was not detected. On fixed tissues, Pon-GFP was detected both around the nucleus and at the cortex of wild-type pI cells. In contrast, endogenous Pon was only detected around the nucleus. Perinuclear Pon colocalized with nuclear-envelope markers such as the MAb414 marker that stained several nuclear-pore antigens and a GFP protein-trap fusion with the ER resident enzyme phospho-di-isomerase (PDI-GFP), which marked the proximal part of the endoplasmic reticulum (ER) (data not shown).

(E) Diagram showing the distribution of the ratio of the following two time periods: the time between the onset of prophase and the onset of anaphase and the time between the Pon-GFP crescent formation and the onset of anaphase.

(F and G) Time-lapse imaging of Pon-GFP (green) and H2B-mRFP (red) expressed under the control of $neur^{PGAL4}$ in wild-type (F) and lgl^{4} mutant (G) pI cells. Time 0:00 corresponds to anaphase. We determined prophase onset by monitoring early chromosome condensation. Upon complete chromosome condensation, we observed a rapid movement of the chromosomes; this rapid movement was probably caused by the nuclear-envelope breakdown, and we defined this point as prometaphase onset. Time is shown in min:s.

(H–K) Two examples of the distribution of Pon-GFP in wild-type (H and I) and lgl^{4} mutant (J and K) pI cells during prometaphase. The panels (H) and (J) correspond, respectively, to the Pon-GFP signal of the –3:45 panel in Figure 2F and the Pon-GFP signal of the –3:51 panel in Figure 2G. Anterior is on the left. The scale bar represents 5 μm.

from the cortex (Figures 2B and 2D). This indicated that Lgl is also needed in interphase to localize Pon-GFP at the cell cortex. This novel phenotype prompted us to compare the distribution of Pon-GFP in wild-type and dividing *lgl* mutant pI cells. As previously reported [4], crescents of Pon-GFP were observed at metaphase in *lgl* mutant, dividing pI cells (n = 46). Nevertheless, the dynamics of Pon-GFP crescent formation as well as Pon-GFP localization were distinct in wild-type and *lgl* mutant pI cells. It was possible to follow the dynamics of Pon-GFP crescent formation in close detail by using Histone2B-mRFP (H2B-mRFP) as a marker of chromatin and mitotic stage. Two distinct time periods were measured in the two-color Pon-GFP/H2B-mRFP movies: the time between the Pon-GFP crescent formation and the onset of anaphase and the time between the onset of prophase and the onset of anaphase. The ratio of these two time periods is close to 1 when the Pon-GFP crescent forms early in prophase, whereas it is close to 0 when the Pon-GFP crescent forms late in metaphase. In wild-type pI cells (n = 23), only 26% of the dividing cells had a time ratio of less than 0.7, whereas the ratio was below 0.7 in 72% of the dividing *lgl* mutant pI cells (n = 25, $p < 0{,}01$, Figure 2E). Representative time-lapse series are shown for dividing wild-type pI cells in Figure 2F (ratio 0.75) and for dividing *lgl* mutant pI cells in Figure 2G (ratio 0.61; the mean value of the wild-type and *lgl* mutant pI cells ratios being 0.76

[n = 23] and 0.62 [n = 25], respectively). Thus, Pon-GFP crescent formation was delayed in *lgl* mutant pI cells relative to wild-type cells.

Furthermore, although Pon-GFP was asymmetrically localized, two additional phenotypes were observed in *lgl* mutant pI cells. First, Pon-GFP was also detected all along the entire pI cell cortex and was not restricted to the anterior cortex from prometaphase to metaphase in 68% of *lgl* mutant pI cells (n = 46, Figures 2H–2K; this was observed in only 12% of the wild-type pI cells at the same stage; n = 30). Second, Pon-GFP was also detected in the cytoplasm from prometaphase to metaphase in 62% of the *lgl* mutant pI cells (n = 46), compared with 12% of the wild-type pI cells at the same stages (n = 30, Figures 2H–2K). In conclusion, Lgl is needed for the prompt and confined formation of the Pon-GFP crescent at the anterior pI cell cortex.

Our time-lapse analysis revealed relatively mild defects in the asymmetric localization of Pon-GFP in *lgl* mutant pI cells. This is in contrast with the strong localization defect seen for endogenous Pon (Figure 1G). Although the basis for this difference remains to be analyzed in detail, it suggests that the overexpression of Pon-GFP is sufficient to bypass the requirement of Lgl for the Pon cortical localization during mitosis. In fact, given that the Pon-GFP crescent forms as the nuclear envelope breaks down, we envisage that an important pool of Pon-GFP is redistributed to the cytoplasm and that the amount of Pon-GFP present in the cytoplasm is sufficient to reach the pI cell cortex. Once at the cell cortex, an unknown Lgl-independent activity can partially restrict Pon-GFP localization to the anterior cell cortex. Finally, our results indicate that, upon overexpression, Pon-GFP is not a faithful reporter of the endogenous Pon localization.

In conclusion, and in contrast to a previous report [4], our results establish that Lgl is needed for the asymmetric localization of cell-fate determinants during pI cell mitosis, as found with Numb and Prospero in neuroblasts [2, 3]. The results indicate that Lgl functions by promoting Pon cortical localization, as found in neuroblasts for Miranda [2, 3].

We next analyzed how *lgl* regulates binary cell-fate decisions in the sensory-organ cell lineage. The *lgl* mutant sensory organs are mostly composed of external sensory cells at the expense of the internal sensory cells because, in part, of the acquisition of a pIIa cell fate by the anterior pI daughter cell ([4] and Figures 3A and 3B). This phenotype was proposed to result from the ectopic activation of Notch signaling in the anterior pI daughter lineage [4], which is otherwise inhibited by Numb in association with α-adaptin [11, 12]. Our results above suggest that the pIIb-to-pIIa cell-fate transformation observed in *lgl* mutant sensory organs may in part result from the reduced amount of Numb inherited by the anterior daughter cell or the segregation of Neur into both pI daughter cells. However, 96% of the *lgl* mutant sensory organs are characterized by a pIIa-to-pIIb cell-fate transformation (n = 37, Figures 3A and 3B), whereas Neur and Numb are mislocalized in only 66% and 60% of pI cells in telophase, respectively. We therefore hypothesized that Lgl also regulates the activity or the localization of additional N regulators that act in parallel or downstream of *numb* during the pIIa-or-pIIb decision. A good candidate is Spdo, as suggested by the following observations. First, *spdo* is required for many, if not all, Numb- and N-mediated binary fate decisions that follow asymmetric cell divisions in the embryo, and loss of *spdo* function results in a pIIa-to-pIIb fate transformation in sensory-organ cell lineage of the embryo [17, 18]. Consistent with this requirement, Spdo is specifically expressed in all precursor cells prior to asymmetric cell divisions in the embryo. Second, as shown for *lgl* [3, 4], *spdo* and *numb* exhibit dosage-sensitive genetic interactions, and in the embryo Spdo acts in parallel to, or downstream of, *numb* to regulate N-dependent binary fate decisions [17, 18]. Third, *spdo* encodes a four-pass transmembrane protein that physically associates with both Numb and N [19]. Spdo predominantly localizes at the plasma membrane of vMP2 (the MP2 neuroblast daughter cell in which N signaling is ON) and in large cytoplasmic punctae in dMP2 (the MP2 daughter cell in which N signaling is OFF). Some of these Spdo-positive punctae also contain N and Dl [19]. Finally, the plasma-membrane localization of Spdo is inhibited by Numb in dMP2, as well as in other neural precursor cells in the embryo [19]. These observations have led to a model in which Spdo localizes at the plasma membrane to allow N signaling and, in addition, Numb prevents N signaling by inhibiting the plasma-membrane localization of Spdo, possibly by promoting the endocytosis of Spdo [19].

To determine whether this model also holds in the pI cell, we first established that loss of *spdo* function leads to a pIIa-to-pIIb cell-fate transformation in the adult mechanosensory-organ lineage (Figures 3C and 3D). We also analyzed the localization of Spdo in the pI cell and its progeny. At interphase, Spdo was present in the cytoplasm of the pI cell (n = 11), where it localized in punctate structures (Figures 3E and 3E′). Some of these Spdo-positive structures were also positive for Dl (not shown) and/or HRS [20] (*h*epatocyte growth factor-*r*egulated tyrosine kinase *s*ubstrate: an endosome-associated, ubiquitin binding protein; data not shown), suggesting that they correspond to endosomes. During the pI cell division, Spdo was more diffusely localized within the cytoplasm, possibly due to the fragmentation of the endocytic compartment at mitosis (n = 15, Figures 3F and 3F′; also 3G and 3G′). After division, Spdo mostly localized into HRS-positive endosomes in the pIIb cell and was not detected at the plasma membrane (Figures 3H–3I′). In contrast, Spdo localized preferentially at the plasma membrane of the posterior pIIa cell (n = 21, Figures 3H–3I′). The analysis of the *numb* mutant pI cells indicated that Numb inhibited the plasma-membrane localization of Spdo in pI cells, both at interphase (n = 13) and during mitosis (n = 14), as well as in pIIb cells (n = 14, Figures 3J–3M). Our analysis of the localization of Spdo in wild-type and *numb* mutant pI daughter cells is consistent with the model in which Numb inhibits the plasma-membrane localization of Spdo, possibly by promoting its endocytosis.

We next investigated whether *lgl* regulates the subcellular localization of Spdo. Spdo was found preferentially localized at the plasma membrane of *lgl* mutant pI cells, both at interphase (n = 14, Figure 3N) and throughout mitosis (n = 13, Figure 3O). Thus, the two pI

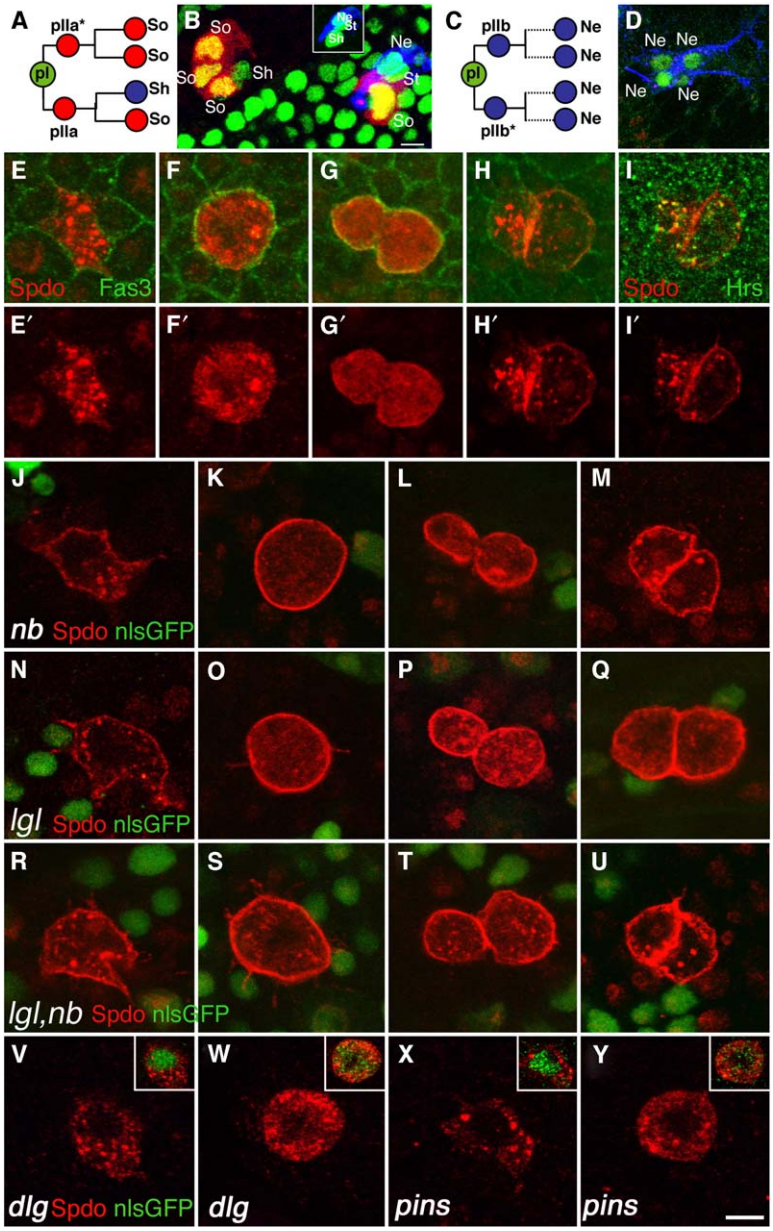

Figure 3. Lgl and Numb Inhibit the Plasma-Membrane Localization of Spdo

(A) Proposed lineage for the *lgl*^{4} mutant pI cell that divides to produce a pIIa and a pIIa-like (pIIa*) daughter cells.

(B and D) *lgl*^{4} ([B], left organ), wild-type ([B], right organ), and *spdo*^{G104} (D) sensory organs at 24 hr after puparium formation (APF) were stained for GFP (green), Cut (green), Su(H) (red), and HRP (blue). Because Cut and nls-GFP staining (green) were both revealed by the same secondary antibody, *lgl* or *spdo* mutant organs were identified within a field of nls-GFP-negative epithelial cells. (B) The wild-type organ (right) is composed of four cells. The subepithelial Su(H)$^{-}$ Cut^{+} shaft cell is located below the Su(H)$^{+}$ socket cell (see inset). The subepithelial Cut^{+} sheath cell is located next to the neuron identified by HRP staining (blue, see inset also). The *lgl* mutant organ (left) is composed of three socket cells identified by Su(H) staining (red) and of a subepithelial Su(H)$^{-}$ Cut^{+} cell identified as a shaft cell based on its large subepithelial polyploid nucleus (not shown). Of the *lgl*^{4} mutant organs, 68% were composed of four socket cells, and the remaining 32% were composed of three socket and one shaft cells (n = 37 *lgl* mutant organs). (D) *spdo*^{G104} mutant sensory organs at 24 hr APF are composed of four subepithelial Cut^{+} and HRP^{+} neurons. Thirty-seven percent of the *spdo*^{G104} mutant pI cells generate four neurons, indicating that these mutant pI cells divided to produce a pIIb and a pIIb-like (pIIb*) daughter cell (n = 19). In the 63% remaining sensory organs, a variable number of neurons was observed. The Su(H)$^{+}$ socket cell was, however, missing in 100% of the *spdo*^{G104} mutant organs.

(C) Proposed lineage for the *spdo*^{G104} mutant pI cell that divides to produce a pIIb and a pIIb-like (pIIb*) daughter cell.

(E–H′) Localization of Spdo (red) and Fas3 (green) in a wild-type pI cell ([E] interphase; [F] prometaphase; [G] telophase) and in pIIa/pIIb cells ([H] interphase).

(I and I′) Localization of Spdo (red) and HRS (green) in wild-type pIIa and pIIb cells. Spdo was specifically detected in the pI cell and in its progeny. It predominantly localized in intracellular puncta in the pI and pIIb cells, where it partially colocalized with HRS. Spdo was not detected at the plasma membrane of the pIIb cell. Spdo accumulated at the plasma membrane in the pIIa cell. Spdo was also found in intracellular dots in the pIIa cell, and some of these dots colocalized with HRS. The nuclear signal detected with the anti-Spdo antibody was a non-specific staining because it was also detected in *spdo*^{ZZ27} mutant cells (not shown).

(J–Y) Localization of Spdo (red) in *numb*^{2} (J–M), *lgl*^{4} (N–Q), *numb*^{2}, *lgl*^{4} (R–U) *dlg*^{1P20} (V and W), or *pins*^{62} (X and Y) mutant pI cells during interphase (J, N, R, V, and X) and at mitosis (K, O, S, W, and Y), as well in pI progeny cells (L, M, P, Q, T, and U). Mutant cells were identified by the loss of nls-GFP staining (green). Sensory cells were identified by Sens staining (not shown in [E–U]; green in insets [V–Y]). Anterior is on the left, and the scale bar represents 5 μm.

daughter cells are born with a high level of Spdo at their plasma membrane (Figure 3P). Furthermore, Spdo remained mostly localized at the plasma membrane in both interphasic pI daughter cells and in *lgl* mutant clones (n = 19, Figure 3Q). In dividing *pins*^{62} mutant pI cells, Numb and Neur failed to localize asymmetrically, similar to what was observed in *dlg*^{1P20} mutant pI cells, where Lgl was cytoplasmic ([10, 13] and data not shown); however, in both interphasic and mitotic pI cells mutant for either *dlg*^{1P20} or *pins*^{62}, the localization of Spdo was not affected (Figures 3V–3Y). We therefore conclude that Lgl inhibits the plasma-membrane localization of Spdo and that this function is independent of Lgl's role in regulating the asymmetric localization of Numb during pI cell division. We propose that the pIIb-to-pIIa fate transformation seen in *lgl* mutant may result from an increased level of Spdo at the plasma membrane of both pI daughter cells, which in turn promotes N signaling

Because the localization of Spdo was similarly affected by the loss of *numb* and *lgl* activity, we wondered whether Numb and Lgl act in the same pathway.

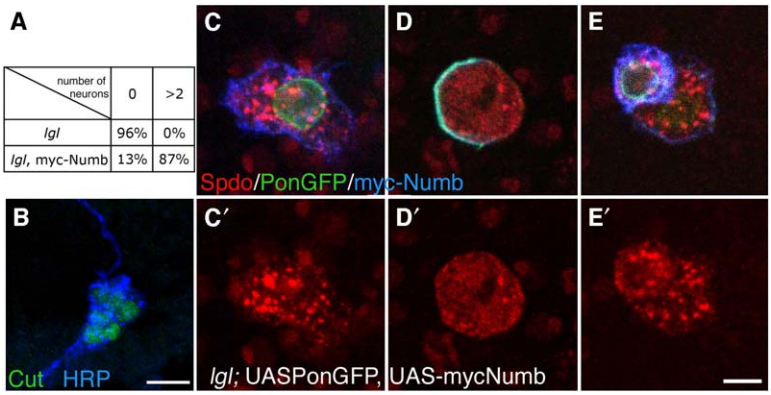

Figure 4. Numb Can Act in a Lgl-Independent Manner to Inhibit the Plasma-Membrane Localization of Spdo

(A) quantification of the number of HRP-positive neurons per sensory organ at 24 hr APF in lgl^4 (*lgl*; n = 37) and lgl^4 mutant sensory organs expressing Myc-Numb (*lgl*, Myc-Numb; n = 32).

(B) lgl^4 mutant sensory organs expressing Myc-Numb under the control of $neur^{PGAL4}$ at 24 hr APF show too many subepithelial Cut- (green) and HRP-positive (blue) neurons. Fifty percent and 37% of the lgl^4 mutant pI cells expressing Myc-Numb generate four and six neurons (as shown in [B]), respectively (n = 32).

(C–E′) Localization of Spdo (red) in lgl^4 mutant pI cells expressing Pon-GFP (green) in combination with Myc-Numb (blue) at interphase (C and C′), in mitosis (D and D′), and in lgl^4 mutant pI progeny cells (E and E′). Expression of Myc-Numb in lgl^4 mutant pI cells inhibits the plasma-membrane localization of Spdo. In contrast, lgl^4 mutant cells expressing Pon-GFP alone exhibit the same phenotype as lgl^4 mutant cells (data not shown). Of note, Myc-Numb colocalized asymmetrically with Pon-GFP in dividing *lgl* mutant pI cells (D). Consistent with this, the amount of Myc-Numb detected in the posterior cell is lower than the one seen in the anterior cell (E). Although it is not clear why overexpressed Myc-Numb behaves differently than endogenous Numb, one possible interpretation is that overexpression of Myc-Numb is sufficient to bypass a requirement of Lgl for Numb cortical localization at mitosis and that, once at the cell cortex, a Lgl-independent activity would partially restrict Numb localization to the anterior cell cortex. Anterior is on the left, and the scale bar represents 10 μm in (B) and 5 μm in (C) and (C′).

We therefore examined the localization of Spdo in double-mutant pI cells. In *lgl,numb* mutant clones, Spdo localized at the plasma membrane of pI cells during interphase (n = 13, Figure 3R) and throughout mitosis (n = 10, Figure 3S) as well as in both pI daughter cells (n = 12, Figures 3T–3U). Importantly, the Spdo cortical-localization defects seen in *lgl,numb* mutant pI cells were not more severe than those seen in cells mutant for either *lgl* or *numb* (compare panels R–U to panels J–M and N–Q in Figure 3). This result is consistent with a model in which Numb and Lgl regulate the same process. To test the epistatic relationship between *numb* and *lgl* for the localization of Spdo, a Myc-tagged version of Numb (Myc-Numb) was overexpressed in *lgl* mutant cells. Overexpression of Myc-Numb in pI cells and in its progeny cells results in pIIa-to-pIIb cell transformation (data not shown and [12, 21, 22]). Interestingly, the majority (87%; n = 32) of *lgl* mutant pI cells expressing Myc-Numb produced multiple neurons at the expense of external cells (Figures 4A and 4B). This indicates that the complete loss of *lgl* function only weakly reduced the activity of Myc-Numb. Thus, in contrast with a previous study [4], we propose that Numb acts downstream of or in parallel to Lgl for the specification of pIIb fate. Furthermore, in contrast with the plasma-membrane accumulation of Spdo in *lgl* mutant cells, Spdo did not accumulate at the plasma membrane of *lgl* mutant cells expressing Myc-Numb. This effect was seen in pI cells during interphase (n = 7, Figures 4C and 4C′) and mitosis (n = 9, Figures 4D and 4D′) as well as in pI daughter cells (n = 10, Figures 4E and 4E′). This subcellular distribution of Spdo is reminiscent to that of Spdo in the pIIb cell and correlates with the pIIa-to-pIIb cell-fate transformations observed in *lgl* mutant pI cells expressing Myc-Numb. Together, these results suggest that Numb functions downstream of Lgl to regulate the plasma-membrane localization of Spdo.

In conclusion, Lgl has at least two distinct functions by which it regulates the fate of its daughter cells during the pI cell cycle. The first function is to promote the cortical recruitment of Pon and the asymmetric localizations of Numb and Neur at the anterior cortex of the dividing pI cell. The second function is to inhibit the plasma-membrane localization of Spdo so that the differential activation of the Notch signaling pathway in the pI daughter cells can occur. Numb appears to act downstream of Lgl to regulate the plasma-membrane localization of Spdo. Thus, for both functions, Lgl appears to act upstream of Numb to regulate Numb localization or activity, or both. The loss of Lgl1 function in mice results in the ectopic expression of the Notch-responding HES5 gene in both sibling neurons after the asymmetric division of brain neural progenitors at E10.5 [23]. Whether this arises through a comparable mechanism remains to be determined because mammalian Spdo functional homologs have yet to be identified.

Experimental Procedures

Flies

lgl^4 is a null *lgl* allele [24]; $pins^{62}$ is null *pins* viable allele [10]; $numb^2$ is a strong loss-of-function *numb* allele. dlg^{1P20} is a hypomorphic *dlg* allele described in [25]. $spdo^{G104}$ is a presumptive null allele of *spdo* containing a single base-pair change introducing a premature stop codon at amino acid 141 [19]. The following UAS, Gal4, or GFP lines were used: $neur^{PGal4}$ [8]; $Scabrous^{PGal4}$ [26]; UAS-Pon-GFP [27]; UAS-DaPKCΔN [1]; UAS-lgl3A [1]; UAS-lgl [1]; HS-Gal4; PDI-GFP [28]; and UAS-Myc-Numb [22]. DNA encoding the human Histone H2B fused to mRFP [29] was cloned as an Acc65I-XbaI fragment into the pUAST vector [16] (details available on request). UAS-H2B-mRFP transgenic lines were generated by DNA injection in *w* strains via the Δ2.3 helper plasmid. lgl^4 clones were recovered from ubx-flp;FRT40A,lgl^4/FRT40A,Ubi-nls-GFP and from ubx-flp; FRT40A,lgl^4/FRT40A,tub-Gal80;neu^{PGal4},UAS-Pon-GFP,UAS-H2B-mRFP/+ pupae. $numb^2$ and $spdo^{G104}$ clones were recovered from HS-flp;FRT40A,$numb^2$/FRT40A,Ubi-nls-GFP and HS-flp;FRT82B, $spdo^{G104}$/FRT82B,Ubi-nls-GFP, respectively. Heat shock was induced at 37°C for 45 min in late L1 larvae. lgl^4 MARCM clones [30] that were positively marked by the neurPGAL4-driven expression of Pon-GFP, either alone or in combination with Myc-Numb, were

recovered from Ubx-flp;FRT40A,*lgl*^{4}/FRT40A,Tub-Gal80;neu^{PGal4},UAS-Pon-GFP/UAS-Myc-Numb.

Immunocytochemistry and GFP Imaging

Pupal nota were dissected from staged pupae and fixed and stained as described in [8]. Primary antibodies were rabbit anti-Pon (gift from Y.N. Jan; 1:1000), rabbit anti-Numb (gift from Y.N. Jan; 1:1000), rabbit anti-Pins (gift from J. Knoblich; 1:1000), rabbit anti-Baz (gift from A. Wodarz; 1:4000), goat anti-PKCzeta (Santa Cruz Biotechnology; 1:1000), goat Cy3-anti-HRP (Sigma; 1:1000), mouse anti-Cut (2B10, obtained from DSHB; 1:1000), rat anti-Su(H) (1:1000), mouse Mab414 (gift from V. Doye; 1:400), mouse anti-GFP (Roche; 1:300), rabbit anti-GFP (Molecular Probes; 1:2000), rabbit anti-Spdo (gift from J. Skeath; 1:1000), mouse anti-Fas3 (7G10, obtained from DSHB; 1:100), guinea pig anti-HRS (gift from H. Bellen; 1:600), rabbit anti-Neur (gift from E. Lai; 1:600), guinea pig anti-Sens (gift from H. Bellen; 1:4000), and mouse anti-Myc (9E10, obtained from DSHB). The Cy3- and Cy5-coupled secondary antibodies were from Jackson Laboratory, and Alexa-488-coupled secondary antibodies were from Molecular Probes. Images were acquired on a Leica SP2 confocal microscope. Live imaging was carried out as described in [8], and images were acquired on a Zeiss LSM510 Meta confocal microscope. Images were processed and assembled with ImageJ and Adobe Photoshop.

Acknowledgments

We thank H. Bellen, R. Bodmer, V. Doye, Y.N. Jan, J. Knoblich, E. Lai, J. Skeath, U. Thomas, A. Wodarz, the Developmental Studies Hybridoma Bank, and the Bloomington Stock Center for strains and antibodies. We also thank the members of the Curie Imaging Facility for help and advice with confocal microscopy. Y.B. thanks A. Morineau for encouragement and support. We thank M. Morgan, N. David, A. Echard, B. Baum, J. Gomes, and A. Bardin for critical reading. This work was supported by grants from the Association pour la Recherche sur le Cancer (ARC 4726 and ARC 7744 to Y.B. and ARC 3415 to F.S), the Fédération pour la Recherche Médicale (Y.B.), the Centre National de la Recherche Scientifique and the Curie Institute (Y.B.), and grants from the Ministry of Research (Action Concertee Incitative program grants to F.S. and Y.B.).

Received: January 14, 2005
Revised: April 18, 2005
Accepted: April 18, 2005
Published: May 24, 2005

References

1. Betschinger, J., Mechtler, K., and Knoblich, J.A. (2003). The Par complex directs asymmetric cell division by phosphorylating the cytoskeletal protein Lgl. Nature *422*, 326–330.
2. Peng, C.Y., Manning, L., Albertson, R., and Doe, C.Q. (2000). The tumour-suppressor genes lgl and dlg regulate basal protein targeting in Drosophila neuroblasts. Nature *408*, 596–600.
3. Ohshiro, T., Yagami, T., Zhang, C., and Matsuzaki, F. (2000). Role of cortical tumour-suppressor proteins in asymmetric division of Drosophila neuroblast. Nature *408*, 593–596.
4. Justice, N., Rogiers, F., Jan, F.Y., and Jan, Y.N. (2003). Lethal giant larvae acts together with numb in notch inhibition and cell fate specification in the Drosophila adult sensory organ precursor lineage. Curr. Biol. *13*, 778–783.
5. Gho, M., and Schweisguth, F. (1998). Frizzled signalling controls orientation of asymmetric sense organ precursor cell divisions in Drosophila. Nature *393*, 178–181.
6. Fichelson, P., and Gho, M. (2003). The glial cell undergoes apoptosis in the microchaete lineage of Drosophila. Development *130*, 123–133.
7. Gho, M., Bellaiche, Y., and Schweisguth, F. (1999). Revisiting the Drosophila microchaete lineage: A novel intrinsically asymmetric cell division generates a glial cell. Development *126*, 3573–3584.
8. Bellaiche, Y., Gho, M., Kaltschmidt, J.A., Brand, A.H., and Schweisguth, F. (2001). Frizzled regulates localization of cell-fate determinants and mitotic spindle rotation during asymmetric cell division. Nat. Cell Biol. *3*, 50–57.
9. Roegiers, F., Younger-Shepherd, S., Jan, L.Y., and Jan, Y.N. (2001). Two types of asymmetric divisions in the Drosophila sensory organ precursor cell lineage. Nat. Cell Biol. *3*, 58–67.
10. Le Borgne, R., and Schweisguth, F. (2003). Unequal segregation of Neuralized biases Notch activation during asymmetric cell division. Dev. Cell *5*, 139–148.
11. Berdnik, D., Torok, T., Gonzalez-Gaitan, M., and Knoblich, J.A. (2002). The endocytic protein α-Adaptin is required for numb-mediated asymmetric cell division in *Drosophila*. Dev. Cell *3*, 221–231.
12. Rhyu, M.S., Jan, L.Y., and Jan, Y.N. (1994). Asymmetric distribution of numb protein during division of the sensory organ precursor cell confers distinct fates to daughter cells. Cell *76*, 477–491.
13. Bellaiche, Y., Radovic, A., Woods, D.F., Hough, C.D., Parmentier, M.L., O'Kane, C.J., Bryant, P.J., and Schweisguth, F. (2001). The Partner of Inscuteable/Discs-large complex is required to establish planar polarity during asymmetric cell division in *Drosophila*. Cell *106*, 355–366.
14. Schaefer, M., Petronczki, M., Dorner, D., Forte, M., and Knoblich, J.A. (2001). Heterotrimeric G proteins direct two modes of asymmetric cell division in the *Drosophila* nervous system. Cell *107*, 183–194.
15. Roegiers, F., Younger-Shepherd, S., Jan, L.Y., and Jan, Y.N. (2001). Bazooka is required for localization of determinants and controlling proliferation in the sensory organ precursor cell lineage in Drosophila. Proc. Natl. Acad. Sci. USA *98*, 14469–14474.
16. Brand, A.H., and Perrimon, N. (1993). Targeted gene expression as a means of altering cell fates and generating dominant phenotypes. Development *118*, 401–415.
17. Dye, C.A., Lee, J.K., Atkinson, R.C., Brewster, R., Han, P.L., and Bellen, H.J. (1998). The Drosophila sanpodo gene controls sibling cell fate and encodes a tropomodulin homolog, an actin/tropomyosin-associated protein. Development *125*, 1845–1856.
18. Skeath, J.B., and Doe, C.Q. (1998). Sanpodo and Notch act in opposition to Numb to distinguish sibling neuron fates in the Drosophila CNS. Development *125*, 1857–1865.
19. O'Connor-Giles, K.M., and Skeath, J.B. (2003). Numb inhibits membrane localization of Sanpodo, a four-pass transmembrane protein, to promote asymmetric divisions in *Drosophila*. Dev. Cell *5*, 231–243.
20. Lloyd, T.E., Atkinson, R., Wu, M.N., Zhou, Y., Pennetta, G., and Bellen, H.J. (2002). Hrs regulates endosome membrane invagination and tyrosine kinase receptor signaling in *Drosophila*. Cell *108*, 261–269.
21. Uemura, T., Shepherd, S., Ackerman, L., Jan, L.Y., and Jan, Y.N. (1989). *numb*, a gene required in determination of cell fate during sensory organ formation in Drosophila embryos. Cell *58*, 349–360.
22. Yaich, L., Ooi, J., Park, M., Borg, J.P., Landry, C., Bodmer, R., and Margolis, B. (1998). Functional analysis of the Numb phosphotyrosine-binding domain using site-directed mutagenesis. J. Biol. Chem. *273*, 10381–10388.
23. Klezovitch, O., Fernandez, T.E., Tapscott, S.J., and Vasioukhin, V. (2004). Loss of cell polarity causes severe brain dysplasia in Lgl1 knockout mice. Genes Dev. *18*, 559–571.
24. Mechler, B.M., McGinnis, W., and Gehring, W.J. (1985). Molecular cloning of lethal(2)giant larvae, a recessive oncogene of Drosophila melanogaster. EMBO J. *4*, 1551–1557.
25. Woods, D.F., Hough, C., Peel, D., Callaini, G., and Bryant, P.J. (1996). Dlg protein is required for junction structure, cell polarity, and proliferation control in Drosophila epithelia. J. Cell Biol. *134*, 1469–1482.
26. Budnik, V., Koh, Y.H., Guan, B., Hartmann, B., Hough, C., Woods, D., and Gorczyca, M. (1996). Regulation of synapse structure and function by the Drosophila tumor suppressor gene *dlg*. Neuron *17*, 627–640.
27. Lu, B., Ackerman, L., Jan, L.Y., and Jan, Y.N. (1999). Modes of protein movement that lead to the asymmetric localization of

partner of Numb during Drosophila neuroblast division. Mol. Cell *4*, 883–891.
28. Morin, X., Daneman, R., Zavortink, M., and Chia, W. (2001). A protein trap strategy to detect GFP-tagged proteins expressed from their endogenous loci in Drosophila. Proc. Natl. Acad. Sci. USA *98*, 15050–15055.
29. Campbell, R.E., Tour, O., Palmer, A.E., Steinbach, P.A., Baird, G.S., Zacharias, D.A., and Tsien, R.Y. (2002). A monomeric red fluorescent protein. Proc. Natl. Acad. Sci. USA *99*, 7877–7882.
30. Lee, T., and Luo, L. (2001). Mosaic analysis with a repressible cell marker (MARCM) for Drosophila neural development. Trends Neurosci. *24*, 251–254.